On the ISAR Image Analysis and Recovery with Unavailable or Heavily Corrupted Data

Ljubiša Stanković, *Fellow IEEE*

Abstract—**Common ISAR radar images and signals can be reconstructed from much fewer samples than the sampling theorem requires since they are usually sparse. Unavailable randomly positioned samples can result from heavily corrupted parts of the signal. Since these samples can be omitted and declared as unavailable, the application of the compressive sensing methods in the recovery of heavily corrupted signal and radar images is possible. A simple direct method for the recovery of unavailable signal samples and the calculation of the restored ISAR image is reviewed. An analysis of the noise influence is performed. For fast maneuvering ISAR targets the sparsity property is lost since the ISAR image is blurred. A nonparametric quadratic time-frequency representations based method is used to restore the ISAR image sparsity. However, the linear relation between the signal and the sparsity domain transformation is lost. A recently proposed gradient recovery algorithm is adapted for this kind of analysis. It does not require the linear relation of the signal and its sparsity domain transformation in the process of unavailable data recovery. The presented methods and results are tested on several numerical examples proving the expected accuracy and improvements.**

Index Terms—**Radar imaging, ISAR, time-frequency analysis, noisy signal, sparse signal, compressive sensing.**

I. INTRODUCTION

In inverse synthetic aperture radar (ISAR) a high resolution image of a target is obtained by using the two-dimensional Fourier transform of the received (and processed) signal. The ISAR image of a point target is a highly concentrated two-dimensional pulse function at a point whose position corresponds to the target's range and cross-range. For a number of reflecting points, the radar image consists of several pulses at the range and cross-positions [1]-[4]. Usually the number (area) of nonzero values in the ISAR image is small as compared to the total number of signal samples. Thus, we may say that the common signal in ISAR is sparse in the two-dimensional Fourier domain [5], [6]. As such it can be reconstructed from much fewer samples than the sampling theorem requires. Unavailable, randomly position samples could also result from heavily corrupted parts of the signal, that are omitted and declared as unavailable, before the ISAR image recovery and calculation is done [7]. In the signal recovery the fact that the two-dimensional Fourier transform domain is the domain of radar signal sparsity is used. This fact allows the application of the compressive sensing methods [5], [6], [8], [9], [23]. A simple method for the unavailable radar signal data recovery and the ISAR image calculation is

Electrical Engineering Department, University of Montenegro, 20000 Podgorica, Montenegro, email: ljubisa@ac.me, www.tfsa.ac.me. Submitted to the IEEE Transactions on Aerospace and Electronic Systems.
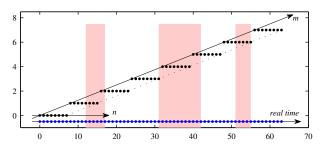
reviewed in the paper. An analysis of the noise influence on this radar image is done. A simple and accurate formula for the output signal-to-noise ratio is derived.

For fast maneuvering ISAR targets, the radar image can be spread over the two-dimensional Fourier transform domain [1], [10]-[18]. Then a large number of the two-dimensional Fourier transform values are nonzero, covering a large part of the radar image. In this case the sparsity property of the signal is lost. One possibility to restore this property is to use parametric transforms to compensate and refocus the ISAR image, making it sparse again [1], [12], [18]. However, a large number of parameters should be used for almost each reflecting point in the case of a general nonuniform motion. Good results can be achieved using these techniques, but at the expense of a high computational load. This kind of parametric calculation is even more complex for the reduced set of available signal samples, when the compressive sensing methods are going to be used. The other way to refocus the image is based on the quadratic time-frequency representations [1], [20]. A representation which can achieve high concentration, like in the Wigner distribution case, at the same time avoiding the cross-terms, is the S-method. This method is nonparametric and computationally quite simple. It requires just a few additional additions and multiplications on the already calculated ISAR image using the two-dimensional Fourier transform [15], [21], [26]. However, the S-method relation to the signal is not linear. Therefore, many conventional compressive sensing based recovery techniques, including the one reviewed in this paper, can not be used. They are based on the direct linear reconstruction relation between the signal and the transform in the domain of signal sparsity. This is not the case in the quadratic signal representations, such as the S-method. It was the reason why the recently proposed gradient method for the signal samples recovery [9] is adapted for the problem formulation in this paper. This method does not require a direct linear relation of the signal and its sparsity transformation domain in the process of recovery of unavailable signal values.

The presented methods and results are illustrated and tested on several numerical examples proving the expected efficiency and improvements.

The manuscript is organized as follows. A brief review of the signal model in the considered ISAR systems is given in Section 2. A reconstruction algorithm for the radar signal with unavailable data is presented in Section 3, along with the analysis of noise influence. The gradient method for the reconstruction of the ISAR images, corresponding to nonuniform motion is presented in Section 4. Examples illustrate the accuracy of the proposed methods.

Fig. 1. Illustration of one revisit (chirp series) discretization in coordinates m (chirp index, slow time) and n (time within one chirp, fast time), along with a real time. The case of $M = 8$ chirps in one revisit and $N = 8$ samples within chirp is presented. The CIT is 64 samples. Unavailable or heavily corrupted data are marked by read.

II. RADAR SIGNAL MODEL

For a continuous wave radar that transmits signal in a form of series of M chirps [1] the received signal (reflected from a target) is delayed with respect to the transmitted signal for $t_d = 2d(t)/c$, where $d(t)$ is the target distance from the radar and c is the speed of light. The received signal, after an appropriate demodulation, compensation and filtering, is

$$q(m,t) = \sigma e^{j\Omega_0 \frac{2d}{c}} e^{-j2\pi B f_r (t - mT_r)\frac{2d}{c}} \quad (1)$$

where σ is the reflection coefficient of the target, while Ω_0 is the radar operating frequency. The repetition time of a single chirp is denoted by T_r, while the number of samples within each chirp is N. The coherent integration time (CIT) is $T_c = MT_r$. Index m corresponds to the chirp index (slow time). The received signal for a system of point scatterers can be modeled as a sum of the individual point scatterer responses, [1]. The Doppler part in the received signal of a point target is

$$s(t) = \sigma e^{j2d(t)\Omega_0/c}, \quad (2)$$

By denoting $t - mT_r = nT_s$, where $T_s = T_r/N$ is a sampling interval within a chirp and n is the index of signal sample within one chirp (fast-time), the range part of the received signal $\exp(-j2\pi B f_r(t - mT_r)\frac{2d}{c})$ reduces to $\exp(j2\pi\gamma n/N)$ with $\gamma = -Bf_r T_s N(2d/c)$. The two-dimensional Fourier transform of the received and processed signal is

$$Q(k,l) = \sum_{m=0}^{M-1}\sum_{n=0}^{N-1} q(m,n)\exp e^{-j(\frac{2\pi mk}{M} + \frac{2\pi nl}{N})}, \quad (3)$$

The illustration of the discrete $q(m,n)$ values in one revisit is presented in Fig. 1.

A. Uniform Target Motion with Unavailable/Corrupted Data

In the simplest case, when the target motion may be considered as uniform within the CIT, the distance can be written as

$$d(t) \cong d_0 + vt \cong d_0 + vmT_r.$$

The received signal, from the ith reflecting point, after the distance compensation, is

$$q_i(m,t) = \sigma_i e^{j\Omega_0 2v_i T_r m/c} e^{j2\pi\gamma_i n/N}$$
$$= \sigma_i e^{j2\pi\beta_i m/M} e^{j2\pi\gamma_i n/N},$$

where β_i and γ_i are the constants proportional to the velocity (cross-range) and range. The total signal for K reflecting points is

$$q(m,n) = \sum_{i=1}^{K} q_i(m,n).$$

Next assume that some blocks of the received radar signal are either unavailable or highly corrupted so that it is better to omit them from the analysis [7]. Assume that the blocks of the omitted signal samples are randomly positioned. The two-dimensional Fourier transform of this signal is then

$$\hat{Q}(k,l) = \sum_{m=0}^{M-1}\sum_{n\in\mathbf{N}_A(m)} q(m,n)e^{-j(\frac{2\pi mk}{M} + \frac{2\pi nl}{N})}.$$

It can happen that the unavailable/corrupted data are: all within one chirp or spread over two or more chirps, including the possibility that a few chirps in a row are affected in this way, Fig. 1. These cases are included by using the notation $n \in \mathbf{N}_A(m)$ where $\mathbf{N}_A(m)$ is the set of available samples within the mth chirp. For some m it could also happen that $\mathbf{N}_A(m) = \varnothing$, i.e., that there are no available samples within that chirp. The total number of available samples is $1 \ll N_A \leq MN$. We can consider two cases [19]:

(1) For $k = \beta_i$ and $l = \gamma_i$ we will have

$$\hat{Q}(k,l) = \sum_{m=0}^{M-1}\sum_{n\in\mathbf{N}_A(m)} \sigma_i = \sigma_i N_A \quad (4)$$

where N_A is the total number of available samples.

(2) For $k \neq \beta_i$ or $l \neq \gamma_i$ then

$$\hat{Q}(k,l) = \sum_{m=0}^{M-1}\sum_{n\in\mathbf{N}_A(m)} \sigma_i e^{j\phi(n,m,k,l)} = \Xi(k,l).$$

For a large number of unavailable samples $1 \ll N_A \ll NM$ the previous value is a sum or vectors with quasi arbitrary phases. It can be considered as a complex-valued variable with Gaussian distributed real and imaginary parts (as shown in [22]). Its variance is

$$\mathrm{var}\{\hat{Q}(k,l)\} = N_A \frac{NM - N_A}{NM - 1}\sigma_i^2.$$

Therefore, for K reflecting points we may write [22]

$$\mathrm{E}\{\hat{Q}(k,l)\} = \sum_{i=1}^{K} \sigma_i N_A \delta(k - \beta_i, l - \gamma_i)$$

$$\mathrm{var}\{\hat{Q}(k,l)\} = N_A \frac{NM - N_A}{NM - 1}\sum_{i=1}^{K} \sigma_i^2 \left(1 - \delta(k - \beta_i, l - \gamma_i)\right).$$

Based on this analysis, the received signal and the ISAR image recovery can be done using the following simple and computationally efficient algorithm.

Algorithm:

(i) Calculate the initial transform estimate $\hat{Q}(k,l)$ by using the available/remaining signal values

$$\hat{Q}(k,l) = \sum_{m=0}^{M-1}\sum_{n\in\mathbf{N}_A(m)} q(m,n)e^{-j(\frac{2\pi mk}{M} + \frac{2\pi nl}{N})}. \quad (5)$$

$$\text{or} \quad \hat{\mathbf{Q}} = \mathbf{\Phi y}.$$

where $\mathbf{y}$ is the vector of available samples $q(m,n)$, $n \in \mathbf{N}_A(m)$

$$\mathbf{y} = [q(m,n)\,|\ \ n \in \mathbf{N}_A(m)]^T.$$

Note that the two-dimensional data $q(n,m)$ are transformed into a column vector $\mathbf{y}$ and $\mathbf{\Phi}$ is the corresponding transformation matrix. It is used to produce $\hat{Q}(k,l)$ arranged into a column vector $\hat{\mathbf{Q}}$.

(ii) Set the resulting transform values $Q(k,l)$ to zero at all positions (k_i, l_i) except the highest $\hat{K}$ values in the initial estimate $\hat{Q}(k,l)$, i.e.,

$$Q(k,l) = 0 \ \ \text{for} \ (k,l) \neq (k_i, l_i), \ i = 1,2,...,\hat{K}$$
$$(k_i, l_i) = \underset{i=1,2,...,\hat{K}}{\arg} \ \{\max\{\text{sort}\{|Q(k,l)|\}\}\}.$$

This criterion is not sensitive to the assumed number of nonzero coefficients $\hat{K}$ as far as all nonzero positions of the original transform are detected and the total number $\hat{K}$ of transform values in $\hat{Q}(k,l)$ is lower than the number of available samples, i.e.,

$$K \leq \hat{K} \leq N_A.$$

All $\hat{K} - K$ transform values that a zero in the original signal will be found as zero-valued in the algorithm.

(iii) The unknown $\hat{K}$ transform coefficients could be then easily calculated by solving the set of N_A equations for available instants $n \in \mathbf{N}_A(m)$, at the detected nonzero candidate positions (k_i, l_i), $i = 1,2,...,\hat{K}$. The linear system for unknowns $Q(k_i, l_i)$ is obtained using the inverse two-dimensional Fourier transform for N_A available signal values,

$$\frac{1}{MN}\sum_{i=1}^{\hat{K}}Q(k_i,l_i)e^{j(\frac{2\pi mk_i}{M}+\frac{2\pi nl_i}{N})} = q(m,n), \qquad (6)$$
$$\text{for} \ 0 \leq m \leq N-1, \quad n \in \mathbf{N}_A(m).$$

System (6) is a system of N_A linear equations with $\hat{K}$ unknown transform values $Q(k_i, l_i)$. This linear system can be written in a matrix form as

$$\mathbf{\Psi}\mathbf{Q}_{\hat{K}} = \mathbf{y},$$

where: $\mathbf{Q}_{\hat{K}}$ is a vector whose elements are unknowns $Q(k_i, l_i)$, $i = 1,2,...,\hat{K}$, $\mathbf{\Psi}$ is the corresponding coefficients matrix, and $\mathbf{y}$ is a vector whose elements are available signal $q(m,n)$ samples.

For $\hat{K} = N_A$ its solution is simple, $\mathbf{Q}_K = \mathbf{\Psi}^{-1}\mathbf{y}$. In general, for $\hat{K} < N_A$ the system is solved in the least square sense as

$$\mathbf{Q}_K = \left(\mathbf{\Psi}^H\mathbf{\Psi}\right)^{-1}\mathbf{\Psi}^H\mathbf{y}. \qquad (7)$$

where H denotes the Hermitian transpose operation. The reconstructed coefficients $Q(k_i, l_i)$, $i = 1,2,...,\hat{K}$, (vector $\mathbf{Q}_{\hat{K}}$) are equal to the transform coefficients of the original signal for all detected candidate frequencies. If some transform coefficients, whose true value should be zero, are included (when $K < \hat{K}$) the resulting system will produce their correct (zero) values.

The condition that the system (6), with $\hat{K}$ unknowns, has a solution is that there are at least $\hat{K}$ independent equations,

i.e., that

$$\text{rank}(\Psi) \geq \hat{K} \ \ \text{or}$$
$$\det(\mathbf{\Psi}^H\mathbf{\Psi}) \neq 0.$$

The reconstruction accuracy can be easily checked calculating the mean squared error between the reconstructed samples and the available samples, at the positions of the available samples $n \in \mathbf{N}_A(m)$.

Comments:

In general, a simple strategy can be used by assuming that $\hat{K} = N_A$ and by setting to zero-value the smallest $N - N_A$ transform coefficients in $\hat{Q}(k,l)$. This simple strategy is very efficient if there is no input noise. Large $\hat{K}$, close or equal to N_A, will increase the probability that full signal recovery is achieved in one step. However, in the case of additional input noise in available samples, a value of $\hat{K}$ as close to the true signal sparsity K as possible will reduce the noise influence on the reconstructed signal. This will be shown later.

If the algorithm fails to detect a component (the reconstruction accuracy of the available samples can be used to detect this event) the procedure can be repeated after the detected components are reconstructed and removed. In such cases the iterative procedure is recommended.

Iterative procedure:

If the number of available samples is low or there are components with much lower amplitudes, so that they can not be detected in one step, the iterative procedure should be used. Algorithm for the iterative procedure is:

-The largest component at (k_1, l_1) in (5) is detected. The transform values $Q(k,l)$ are set to zero at all positions (k,l) except at the position of the highest one at (k_1, l_1). This component is reconstructed using (6) with $\hat{K} = 1$ and subtracted from the signal.

-The remaining signal is used to calculate (5) again. The highest value position (k_2, l_2) is found, and signal is reconstructed at two frequency points $\{(k_1, l_1), (k_2, l_2)\}$ using (6) with $\hat{K} = 2$. The reconstructed signal is removed from the original signal and (5) is calculated with the remaining signal.

-Procedure is continued in this way until the maximal absolute difference of the reconstructed signal, with $\hat{K}$ components at positions $\{(k_1, l_1), (k_2, l_2), ..., (k_{\hat{K}}, l_{\hat{K}})\}$, and the given available signal values (at the positions $n \in \mathbf{N}_A(m)$) is bellow the required accuracy level.

Example 1: A signal with $K = 10$ randomly positioned reflecting points

$$q(m,n) = \sum_{i=1}^{10} \sigma_i e^{j2\pi\beta_i m/M} e^{j2\pi\gamma_i n/N},$$

with reflecting coefficients $1/8 \leq \sigma_i \leq 3/8$ and $M = N = 64$ is considered with 87.5% unavailable samples. The two-dimensional Fourier transform (ISAR image) of the original signal, if all signal samples were available, is presented in Fig.2(a). The initial two-dimensional Fourier transform of the signal is calculated using (5) with $N_A = 0.125MN$ available samples, Fig.2(b). It is presented in Fig.2(c). The largest $\hat{K} =$
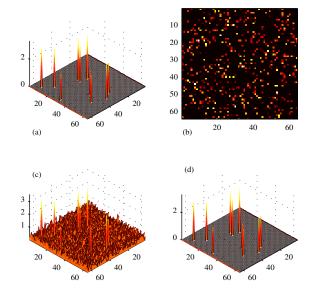
Fig. 2. (a) A two-dimensional Fourier transform of the considered radar signal (ISAR image). (b) Radar signal with 12.5% of available/uncorrupted samples (unavailable/corrupted samples are presented in black). (c) The two-dimensional Fourier transform calculated using the available samples of the radar signal. (d) The recontracted ISAR image.

$14 > 10$ values in $\hat{Q}(k,l)$ are taken as candidates for the nonzero coefficients. Note that any $10 \leq \hat{K} \leq 512$ would produce the same result, as far as the nonzero coefficients of the original signal's two-dimensional Fourier transform are included. The signal is then fully reconstructed using (6)-(7) and presented in Fig.2(d). The difference between the available signal values and the reconstructed signal values, at the same positions, is within the computer precision.

B. Influence of Additive Input Noise

Assume now that an input additive noise $\varepsilon(n)$ exists in the available data. Note that the noise due to missing values influences the results in the sense presented in the previous section. When the recovery is achieved the accuracy of the result is related to the input additive noise in signal samples. It also depends on the number of available signal samples and nonzero transform coefficients (sparsity) as it will be shown next.

The reconstruction equations (6) for the noisy available data are

$$q(m,n) + \varepsilon(m,n) = \frac{1}{MN}\sum_{i=1}^{\hat{K}} Q(k_i,l_i)e^{j(\frac{2\pi mk_i}{M} + \frac{2\pi nl_i}{N})},$$
(8)

$$\text{for } 0 \leq m \leq N-1, \quad n \in \mathbf{N}_A(m).$$

The transform indices can take a value from the set of detected values $(k,l) \in \{(k_1,l_1),(k_2,l_2),...,(k_{\hat{K}},l_{\hat{K}})\}$. A matrix form of equations (8) is

$$\mathbf{y} + \varepsilon = \mathbf{\Psi}\mathbf{Q}_{\hat{K}}.$$

This is a system of N_A linear equations with $\hat{K}$ unknowns in $\mathbf{Q}_{\hat{K}}$. As it has been shown, the solution is

$$\mathbf{\Psi}^H(\mathbf{y} + \varepsilon) = \mathbf{\Psi}^H\mathbf{\Psi}\mathbf{Q}_{\hat{K}}$$
$$\mathbf{Q}_{\hat{K}} = \left(\mathbf{\Psi}^H\mathbf{\Psi}\right)^{-1\mathbf{\Psi}H}(\mathbf{y}+\varepsilon)$$
$$\mathbf{Q}_{\hat{K}} = \mathbf{Q}_{KS} + \mathbf{Q}_{KN}.$$
(9)

The true transform coefficients and the noise influence to the reconstructed transform are

$$\mathbf{Q}_{KS} = \left(\mathbf{\Psi}^H\mathbf{\Psi}\right)^{-1}\mathbf{\Psi}^H\mathbf{y},$$
$$\mathbf{Q}_{KN} = \left(\mathbf{\Psi}^H\mathbf{\Psi}\right)^{-1}\mathbf{\Psi}^H\varepsilon.$$

If all signal samples were available, the input signal-to-noise (SNR) ratio, would be

$$SNR_i = 10\log\frac{\sum_{m=0}^{M-1}\sum_{n=0}^{N-1}|q(m,n)|^2}{\sum_{m=0}^{M-1}\sum_{n=0}^{N-1}|\varepsilon(m,n)|^2} = 10\log\frac{E_s}{E_\varepsilon}.$$
(10)

Assume that the noise energy in the available samples is

$$E_{\varepsilon A} = \sum_{m=0}^{M-1}\sum_{n\in\mathbf{N}_A}|\varepsilon(m,n)|^2.$$
(11)

The true amplitude in the signal transform at the position (k_i,l_i), in the case if all signal samples were used, would be $MN\sigma_i$ where σ_i is the amplitude (reflection coefficient) of the signal component corresponding to the position (k_i,l_i). To compensate the resulting transform for the known bias in amplitude (4) when only N_A available samples are used the coefficient should be multiplied by MN/N_A. In a full recovery, a signal transform coefficient is equal to the coefficient of the original signal with all signal samples being used. The noise in the transform coefficients is multiplied by the same factor of MN/N_A. Therefore, the energy of noise in the reconstruction algorithm is increased to $E_{\varepsilon A}(MN/N_A)^2$. The SNR in the recovered signal is

$$SNR = 10\log\frac{\sum_{m=0}^{M-1}\sum_{n=0}^{N-1}|q(m,n)|^2}{\frac{M^2N^2}{N_A^2}\sum_{m=0}^{M-1}\sum_{n\in\mathbf{N}_A}|\varepsilon(m,n)|^2}$$
(12)

Since only $\hat{K}$ out of MN coefficients are used in the reconstruction the energy of the reconstruction error is reduced for the factor of $\hat{K}/(MN)$ as well. The energy of noise in the recovered signal is

$$E_{\varepsilon R} = \frac{\hat{K}}{MN}\frac{M^2N^2}{N_A^2}\sum_{m=0}^{M-1}\sum_{n\in\mathbf{N}_A}|\varepsilon(m,n)|^2.$$

The SNR in the recovered signal is

$$SNR = 10\log\frac{\sum_{m=0}^{M-1}\sum_{n=0}^{N-1}|q(m,n)|^2}{\frac{\hat{K}NM}{N_A^2}\sum_{m=0}^{M-1}\sum_{n\in\mathbf{N}_A}|\varepsilon(m,n)|^2}.$$
(13)

Since the variances of noise in all samples and the available samples are the same then

$$\frac{1}{N_A}\sum_{m=0}^{M-1}\sum_{n\in\mathbf{N}_A}|\varepsilon(m,n)|^2 = \frac{1}{MN}\sum_{m=0}^{M-1}\sum_{n=0}^{N-1}|\varepsilon(m,n)|^2 \quad (14)$$

Thus, the SNR in the recovered signal, according to (13), (14) and (10), is

$$SNR = SNR_i - 10\log\left(\frac{\hat{K}}{N_A}\right). \qquad (15)$$

We may conclude that in the case of additive input noise in the available signal samples, the output SNR will be increased if the number $\hat{K}$ is as small as possible, for a given number of available samples N_A. In the ideal case, with respect to the additive noise, value of $\hat{K}$ should be equal to the signal sparsity $\hat{K} = K$.

Example 2: Consider a noisy signal from Example 1. Assume that an additive complex-valued Gaussian noise exists, with the input SNR equal to

$$SNR_i = 9.05 \text{ [dB]}$$

and $N_A = MN/8$. Since $K = 10$ in the previous example we used estimated value $\hat{K} = 14$ for the calculation. According to (15) the output SNR is

$$SNR = SNR_i - 10\log\left(\frac{\hat{K}}{N_A}\right)$$
$$= 9.05 + 15.81 = 24.86 \text{ [dB]}.$$

The improvement in SNR is 15.81 [dB]. This result is statistically checked. The statistical result is obtained by averaging over 100 realizations. The obtained statistical value of the output SNR is

$$SNR^{(stat)} = 24.53 \text{ [dB]}.$$

Agreement with the theory is almost exact, within the number of realizations statistical confidence.

If the number of components was estimated exactly as $\hat{K} = 10$, then the SNR values would be obtained as

$$SNR = 26.32 \text{ [dB]}$$
$$SNR^{(stat)} = 26.26 \text{ [dB]}.$$

The SNR value for $\hat{K} = 10$ would be higher for $10\log(14/10) = 1.46$ [dB] than in the case with $\hat{K} = 14$.

C. Nonuniform Target Motion

For fast moving targets and complex motions, the target over all M chirps, in one revisit, cannot be considered as the one with constant velocity motion. Then a higher-order approximation

$$d(t) \cong d_0 + v_0 t + a\frac{t^2}{2} + \ldots,$$

should be used with

$$v(t) = v_0 + at + \ldots$$

If we assume that $v(t) = v_0 + at$, then the Doppler shift is linear function of time. Its rate is a. Thus, instead of a delta pulse concentrated at one frequency, corresponding to v_0, we will obtain a Fourier transform of a linear frequency-modulated signal (or higher-order frequency-modulated signal), whose instantaneous frequency changes are proportional

to the velocity $v(t)$ changes. The radar image, based on this form, is centered at the same position as the Fourier transform image, but with the spreading term in the cross-range (Doppler) direction of the form $\exp\left(j\frac{2\Omega_0}{c}\left(\frac{1}{2!}d''(0)t^2 + \ldots\right)\right)$, due to the target motion. In the discrete domain the signal is [15]

$$q_i(m,n) = \sigma_i e^{j2\pi\beta_i m/M} e^{j\alpha_i m^2/2 + \cdots} e^{j2\pi\gamma_i n/N},$$
$$Q_i(k,l) = (2\pi)^2 \sigma_i \delta(k - \beta_i, l - \gamma_i) *_k \text{FT}\{e^{j\alpha_i m^2/2 + \cdots}\}$$

where $\alpha_i = 2\Omega_0 T_r^2 d''(0)/c$ and $*_k$ is the convolution in the discrete cross-range domain. This spread can be significant and the resulting ISAR image is not sparse or sparsity is significantly degraded.

If the two-dimensional Fourier transform is corrected according to the S-method [15], [21], [26], along the cross-range direction, then the resulting image will be

$$SM_i(k,l) = (2\pi)^2 \sigma_i^2 \delta(k - \beta_i, l - \gamma_i).$$

It is sparse again and does not depend on $d''(0)$. Under certain conditions this representation is free of cross-terms among different reflection points, producing

$$SM(k,l) = (2\pi)^2 \sum_{i=1}^{K} \sigma_i^2 \delta(k - \beta_i, l - \gamma_i).$$

The S-method based ISAR image can be easily realized in a recursive way starting from

$$SM_0(k,l) = |Q(k,l)|^2, \qquad (16)$$

with $SM_0(k)$ being the standard two-dimensional Fourier transform based radar image. The S-method based presentation can be achieved starting with the already obtained Fourier transform-based radar image $Q(k,l)$, with an additional simple calculation according to

$$SM_L(k,l) = SM_{L-1}(k,l) + 2\operatorname{Re}\{Q(k+L,l)Q^*(k-L,l)\}$$

or

$$SM_L[q(m,n)] = SM_L(k,l) \qquad (17)$$
$$= |Q(k,l)|^2 + 2\sum_{z=1}^{L} \operatorname{Re}\{Q(k+z,l)Q^*(k-z,l)\}$$

In this way, using the S-method, we will restore signal sparsity in the ISAR image domain. However we have lost the possibility to use a direct linear relation between the signal and the sparsity domain transformation. For a reduced set of $N_A < MN$ available signal samples, $n \in \mathbf{N}_A(m)$ the problem statement is now

$$\min \|SM_L(k,l)\|_0 \text{ subject to the available values } \mathbf{y}. \quad (18)$$

where $\mathbf{y}$ is the vector of the available signal samples $q(m,n)$, $n \in \mathbf{N}_A(m)$ and

$$\|SM_L(k,l)\|_0 = \sum_{k=0}^{N-1} \sum_{l=0}^{N-1} |SM_L(k,l)|^0.$$

The simple counting of nonzero coefficients by using the zero-norm with $|SM(k,l)|^0$ is, in theory, the best optimization

function. Finding the unavailable signal value to produce the minimal number of nonzero coefficients in the resulting presentation is an obvious optimization criterion. However, this criterion is very sensitive to small values in $SM_L(k,l)$. Also the gradient solutions are not possible with the zero-norm functions, since they are completely flat for any nonoptimal value. That is why the norm-one is used in the standard compressive sensing methods instead of the norm-zero. In the S-method formulation the norm that will correspond to the commonly used norm-one of the Fourier transform is

$$\min \|SM_L(k,l)\|_{1/2} \text{ subject to available values of } \mathbf{y}. \quad (19)$$

with

$$\|SM_L(k,l)\|_{1/2} = \sum_{k=0}^{N-1} \sum_{l=0}^{N-1} |SM_L(k,l)|^{1/2}.$$

This form, for $L = 0$ reduces to the norm-one of the Fourier transform, since

$$\sum_{k=0}^{N-1} \sum_{l=0}^{N-1} |SM_0(k,l)|^{1/2} = \sum_{k=0}^{N-1} \sum_{l=0}^{N-1} |Q(k,l)| = \|Q(k,l)\|_1$$

Minimization of $\sum_{k=0}^{N-1} \sum_{l=0}^{N-1} |SM_L(k,l)|^{1/2}$ has already been used for the time-frequency parameters optimization in [24]. Note that under certain conditions the norm-one produces the same result as the norm-zero in the problem formulation (18), [5], [6].

A simple gradient algorithm to iteratively calculate the missing signal values, while keeping available samples $q(m,n)$ unchanged, [9], is adapted for the problem formulation (19). It is presented next.

D. Algorithm

This gradient algorithm is inspired by the adaptive signal processing methods with an adaptive step size. It is a gradient descent algorithm where the missing samples, are corrected according to the gradient of the sparsity measure $\|SM_L(k,l)\|_{1/2}$. Their final value should converge to the point of the minimal sparsity measure of the signal time-frequency representation.

The algorithm for missing samples reconstruction is implemented as follows:

Step 0: Set $s = 0$, $p = 0$ and form the initial signal $y^{(0)}(m,n)$ defined for all m and n as:

$$y^{(0)}(m,n) = \begin{cases} q(m,n) & \text{for available samples, } n \in \mathbf{N}_A(m) \\ 0 & \text{for } n \notin \mathbf{N}_A(m) \end{cases}$$

The initial value for an algorithm parameter Δ is estimated as

$$\Delta = \max_{n \in \mathbf{N}_A(m)} |q(m,n)|. \quad (20)$$

Step 1: Set $y_r(m,n) = y^{(p)}(m,n)$. This signal is used in Step 3 in order to estimate reconstruction precision.
Step 2.1: Set $p = p + 1$. For each missing sample at (n_i, m_i) for $n \notin \mathbf{N}_A(m)$ form the signals $y_1(m,n)$ and $y_2(m,n)$:

$$y_1(m,n) = y^{(p)}(m,n) + \Delta\delta(n - n_i, m - m_i)$$
$$y_2(m,n) = y^{(p)}(m,n) - \Delta\delta(n - n_i, m - m_i). \quad (21)$$

Step 2.2: Estimate differential of the signal transform measure

$$g(m_i, n_i) = \frac{\|SM_{1,L}(k,l)\|_{1/2} - \|SM_{2,L}(k,l)\|_{1/2}}{2N\Delta} \quad (22)$$

where $SM_{1,L}(k,l) = \text{SM}_L[y_1(m,n)]$ and $SM_{2,L}(k,l) = \text{SM}_L[y_2(m,n)]$ are the S-methods of $y_1(m,n)$ and $y_2(m,n)$, respectively, calculated with L correction terms.
Step 2.3: Form a gradient matrix $\mathbf{G}_p$ with the same size as the signal $q(m,n)$. At the positions of available samples $n \in \mathbf{N}_A(m)$, this vector has value $G_p(m,n) = 0$. At the positions of missing samples $n_i \notin \mathbf{N}_A(m)$ its values are $G_p(m,n) = g(m_i, n_i)$, calculated by (22).
Step 2.4: Correct the values of $y(m,n)$ iteratively by

$$y^{(p)}(m,n) = y^{(p-1)}(m,n) - 2\Delta G_p(m,n), \quad (23)$$

Step 3: If the maximal allowed number of iterations $P_{\max}$ is reached stop the algorithm. Otherwise calculate

$$T_r = \frac{\sum_{m=0}^{M-1} \sum_{n \notin \mathbf{N}_A} |y_r(m,n) - y^{(p)}(m,n)|^2}{\sum_{m=0}^{M-1} \sum_{n \notin \mathbf{N}_A} |y^{(p)}(m,n)|^2}.$$

Value of T_r is an estimate of the reconstruction error to signal ratio, calculated for missing samples only. If T_r is above the required precision threshold (for example, if $T_r > 0.001$), the calculation procedure should be repeated with smaller Δ. For example, set new Δ value as $\Delta/\sqrt{10}$, increment the step counter $s = s + 1$, and go to **Step 1**.
Step 4: Reconstruction with the required precision is obtained in p iterations or when the maximal allowed number of iterations $P_{\max}$ is reached. The reconstructed signal is $\hat{q}(m,n) = y(m,n) = y^{(p)}(m,n)$.

By performing presented iterative procedure, the missing values will converge to the true signal values, producing the minimal sparsity measure in the ISAR image domain.

Comments on the algorithm:
- Inputs to the algorithm are the signal size $M \times N$, set of available signal samples $\mathbf{N}_A$, available signal values $q(m_i, n_i)$, $n_i \in \mathbf{N}_A(m)$, the maximal allowed number of iterations $P_{\max}$ and the required precision used in **Step 3**. The algorithm output is the reconstructed signal matrix $q(m,n) = y(m,n)$.
- When we approach to the optimal point, the gradient algorithm using the norm-one and a large number of variables (missing signal values) will produce a solution close to the exact signal samples, with a precision related to the algorithm step Δ. The precision is improved by using adaptive step Δ. A value of Δ equal to the signal magnitude (20) is used in the starting iteration. When the optimal point is reached then, due to the norm-one like form, the algorithm will not improve the reconstruction precision any more, for a given algorithm step Δ. When this case (in Step 3) is detected the step Δ is reduced, and the same calculation procedure is continued from the reached reconstructed signal values. In several steps, the algorithm can approach the true signal values with a required precision.
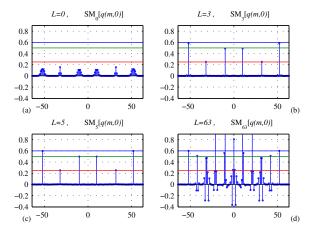
Fig. 3. All signal samples (chirps) available: (a) The Fourier transform based presentation. (b) The S-method with three correction terms, $L = 3$. (c) The S-method with five correction terms, $L = 5$. (d) The Wigner distribution based presentation (the S-method with $L = 63$). Horizontal lines (red, green, blue) present the level of the true squared amplitudes of the components.
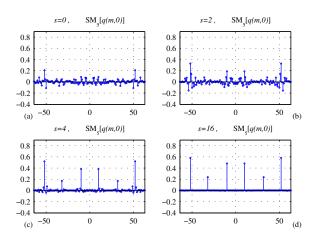
Fig. 4. The S-method presentation (radar image) with missing/corrupted 1/3 of the signal samples (chirps): (a) Initial S-method personation $p = 0$, and the reconstructed S-method in the next iterations (b)-(d) with $p = 2$, $p = 4$, and $p = 16$, respectively.

Example 3: A signal corresponding to the Doppler part of radar signal only is considered first. Its form is

$$q(m, 0) = \sum_{i=1}^{6} \sigma_i e^{j2\pi\beta_i m/M} e^{j\alpha_i m^2/2}$$
$$= 2\sqrt{0.6} \cos(52m\pi/64 - 2.2\pi(m/64)^2)$$
$$+ 2\sqrt{1/2} \cos(10m\pi/64 + 2\pi(m/64)^2)$$
$$+ 2\sqrt{1/4} \cos(32\pi m/64 - 0.75\pi(m/64)^2)$$

with $-64 \leq m \leq 63$ and $\sigma_i \in \{\sqrt{0.6}, \sqrt{0.6}, \sqrt{0.5}, \sqrt{0.5}, \sqrt{0.25}, \sqrt{0.25}\}$, $\beta_i \in \{26, -26, 5, -5, 16, -16\}$ and $\alpha_i \in \{-1.1\pi/1024, 1.1\pi/1024, \pi/1024, -\pi/1024, -0.375\pi/1024, 0.375\pi/1024\}$, for $i = 1, 2, ..., 6$. The representations with all available samples are presented in Fig.3. The Fourier transform base presentation (radar image) is shown in Fig.3(a) for $L = 0$ since $SM_0(k, 0) = |Q(k, 0)|^2$. We can see that although there are just 6 reflecting points the number of nonzero (significant) values in $SM_0(k)$ is above 40. The sparsity condition is heavily degraded. Adding just a few of the correction terms, according to (17), and calculating the S-method based presentation the sparsity in ISAR image is restored. Presentations with $L = 3$ and $L = 5$ in the S-method are shown in Fig.3(b)-(c). Note that the Wigner distribution, $WD(k, 0) = SM_{63}(k, 0)$, although well concentrated for the components, can not be used due to emphatic cross-terms which degrade the sparsity, Fig.3(d).

Consider next the signal with 45 missing signal values (missing chirps in this case). Here, the S-method is calculated with $L = 5$ and the gradient based reconstructed algorithm is applied. The S-method, assuming all missing values are set to 0, is presented for the initial iteration in Fig.4(a). The next iterations steps according to the presented iterative algorithm (denoted by step counter s), improve the presentation toward the case as if all data were available, Fig.4(b)-(d) for $s = 2, 4$, and 16.

Example 4: The setup that will be considered for this ISAR example assumes [25]: a high-resolution radar operating at the frequency $f_0 = 10.1$ GHz, $\Omega_0 = 2\pi f_0$, bandwidth of linear frequency-modulated chirps $B = 300$ MHz, and the coherent integration time $T_c = 2$ s. The pulse repetition time is $T_r = T_c/256$ with the sampling interval $T_s = T_r/64$. The target is at 2 km distance from the radar, and rotates at $\Omega_R = 4\pi/180 \, 1/s = 4°/s$. The nonlinear rotation with frequency $\Omega = \pi \, 1/s$ is superimposed, $\Omega_R(t) = \Omega_R + A\sin(\Omega t)$, and amplitude $A = 1.25\pi/180 \, 1/s$ corresponds to the total change in angular frequency Ω_R for $2.5\pi/180 \, 1/s$. Note that here the range and the cross-range resolutions are $R_{\text{range}} = c/(2B) = 0.5$ m, and $R_{\text{cross-range}} = \pi c/(\Omega_0 T_c \Omega_R) = 0.106$ m (calculated for $T_c = 2$ s with $\Omega_R \cong 4\pi/180 \, 1/s$, neglecting effects of the nonlinear rotation). It has been assumed that there are 15 reflecting points at the positions $(x_i, y_i) \in \{(-3.5, -3.5), (-3.5, -0.5), (-3.5, 2.5), (0, -3), (0, 0), (0, 3), (2.5, -3), (2.5, 0), (2.5, 3.5), (3.5, -1.5), (3.5, 2.5), (-2, 2), (-2, -3), (5, 0.5), (5, 3)\}$. First, the case with all available data is considered. The ISAR image based on the two-dimensional Fourier transform is presented in Fig.5(a). The S-method based ISAR image with $L = 3$ and $L = 6$ is shown in in Fig.5(b)-(c). It can be seen that just a few correction terms to the Fourier transform based ISAR image significantly improve the concentration. The Wigner distribution (the S-method with $L = 64$) is highly concentrated. However it suffers from the cross-terms, Fig.5(d). The range and cross-range coordinate axes are scaled with the resolution parameters.

The case with 50% of the data being unavailable (or removed due heavy corruption) is considered next. The ISAR image calculated by using the two-dimensional Fourier transform is presented in Fig.6(a). As we can see the image sparsity is low. Since a large amount of the data is missing this image can not be improved by a direct application of the S-method since the missing data behave as a noise (Section II.A). The S-method based image with $L = 6$ is shown in Fig.6(b). The same holds for the Wigner distribution (the S-method with $L = 64$) given in Fig.6(c). However, the original
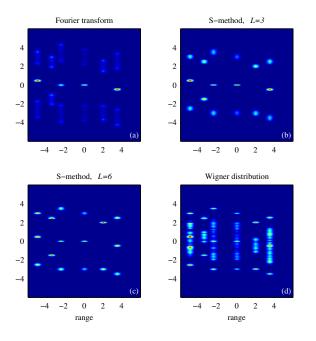
Fig. 5. The ISAR image based on: (a) The two-dimensional Fourier transform. (b) The S-method with $L = 3$. (c) The S-method with $L = 6$. (d) The Wigner distribution (the S-method with $L = 64$). All data are available.
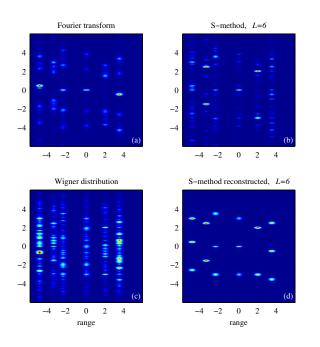

Fig. 6. The ISAR image based on: (a) The two-dimensional Fourier transform. (b) The S-method with $L = 6$. (c) The Wigner distribution. (d) The S-method based on the reconstructed signal in two steps ($s = 2$). Only 50% of randomly positioned available data are used in the reconstruction.

image calculated with the S-method is highly sparse. Therefore the unavailable data can be reconstructed by minimizing the S-method subject to the available data, equation (19). The gradient based method is used to solve this minimization problem. The reconstructed S-method is almost the same as the S-method of the signal with all available data. It is presented in Fig.6(d).

III. CONCLUSION

An analysis of the ISAR image reconstruction in the case of a large number of unavailable or heavily corrupted data is presented. A simple method that can produce reconstruction in the case of uniform motion is reviewed, along with a simple an accurate analysis of the noise influence to the results. In the case of fast and complex target manoeuvring the ISAR image is blurred and the sparsity property is lost. For a large number of reflecting points a parametric approach to refocus the image and reconstruct the signal with large number of missing data would be computationally extensive. A simple nonparametric method is used here to refocus image. Since it belongs to the class of quadratic time-frequency representations, a direct linear relation between the sparsity domain and the signal can not be established. Thus, the reconstruction task is appropriately reformulated. An adapted form of gradient algorithm is used is recover the ISAR image of the quality as in the case if all data were available. The efficiency of the proposed methods is illustrated on several numerical examples.

REFERENCES

[1] V. C. Chen, H. Ling: *Time-frequency transforms for radar imaging and signal analysis*, Artech House, Boston, USA, 2002.
[2] LJ. Stanković, M. Daković, and T. Thayaparan, *Time-Frequency Signal Analysis with Applications*. Artech House, Boston, March 2013
[3] F. Totir and E. Radoi: "Superresolution algorithms for spatial extended scattering centers," *Digital Signal Processing,* Vol. 19, No. 5, pp.780-792, Sept. 2009.
[4] M. Martorella: "Novel approach for ISAR image cross-range scaling," *IEEE Trans. Aerosp. Electron. Syst.*, Vol. 44, No. 1, pp. 281–294, 2008.
[5] D. L. Donoho, "Compressed sensing," *IEEE Transactions on Information Theory*, vol. 52, no. 4, pp. 1289–1306, 2006.
[6] E. J. Candès, J. Romberg, and T. Tao, "Robust uncertainty principles: Exact signal reconstruction from highly incomplete frequency information," *IEEE Trans. on Information Theory*, vol. 52, no. 2, pp. 489–509, 2006.
[7] L. Stanković, S. Stanković, I. Orović, and M. Amin, "Robust Time-Frequency Analysis based on the L-estimation and Compressive Sensing," *IEEE Signal Processing Letters*, Vol. 20, No. 5, pp. 499-502.
[8] M. A. Figueiredo, R. D. Nowak, and S. J. Wright, "Gradient projection for sparse reconstruction: Application to compressed sensing and other inverse problems,"*IEEE Journal of Selected Topics in Signal Processing,*, vol. 1, no. 4, pp. 586–597, 2007.
[9] L. Stanković, M. Daković, and S. Vujović, "Adaptive Variable Step Algorithm for Missing Samples Recovery in Sparse Signals," *IET Signal Processing*, Volume 8 , no. 3, May 2014, pp.246-256.
[10] M. Martorella and F. Berizzi: "Time windowing for highly focused ISAR image reconstruction," *IEEE Trans. Aerosp. Electron. Syst.*, Vol. 41, No. 3, pp. 992–1007, 2005.
[11] F Berizzi, M Martorella, A Cacciamano, A Capria, "A contrast-based algorithm for synthetic range-profile motion compensation," *IEEE Trans. Geosci. Remote Sens.* 46, 3053–3062 (2008)
[12] I. Djurovic, T. Thayaparan, L. Stankovic, "Adaptive Local Polynomial Fourier Transform in ISAR", *EURASIP Journal on Applied Signal Processing*, Vol. 2006, Article ID 36093, 2006.
[13] J.H. Park and N.H. Myung, "Enhanced and efficient ISAR image focusing using the discrete gabor representation in an oversampling scheme," Progress In Electromagnetics Research, Vol. 138, 227-244, 2013.
[14] Shin, S. Y. and N. H. Myung, "The application of motion compensation of ISAR image for a moving target in radar target recognition," *Microwave and Optical Technology Letters*, Vol. 50, No. 6, 1673-1678, 2008..
[15] L. Stankovic, T. Thayaparan, V. Popovic, I. Djurovic, M. Dakovic, "Adaptive S-Method for SAR/ISAR Imaging", *EURASIP Journal on Advances in Signal Processing,* Vol. 2008.
[16] R. Li , J. Tao and W. D. Shi, "Time selection for ISAR imaging based on time-frequency analysis", *Proc. SPIE 8768, International Conference on Graphic and Image Processing (ICGIP 2012)*, 87682V (March 20, 2013); doi:10.1117/12.2010913;

[17] Y. Wang and Y.-C. Jiang: "ISAR imaging of ship target with complex motion based on new approach of parameters estimation for polynomial phase signal," *EURASIP Journal on Advances in Signal Processing*, Vol. 2011 (2011), Article ID 425203, 9 pages.

[18] S.B. Peng, J. Xu, Y.N. Peng, J.B. Xiang, "Parametric inverse synthetic aperture radar maneuvering target motion compensation based on particle swarm optimizer," *IET Radar Sonar Navigat.* 5, 305–314 (2011).

[19] L. Stanković, M. Daković, T. Thayaparan, and V. Popović-Bugarin, "Micro-Doppler Removal in the Radar Imaging Analysis," IEEE Transactions on Aerospace and Electronic Systems, Vol. 49, No. 2, April 2013, pp.1234-1250.

[20] Y. Wang, H. Ling, and V. C. Chen, "ISAR motion compensation via adaptive joint time-frequency techniques," *IEEE Trans. Aerosp. Electron. Syst.*, Vol. 38, No. 2, pp. 670-677, 1998.

[21] L. Stanković, "A method for time-frequency signal analysis," *IEEE Transactions on Signal Processing*, Vol-42, No.1, Jan.1994.pp.225-229.

[22] L. Stanković, S. Stanković, and M. G. Amin, "Missing Samples Analysis in Signals for Applications to L-Estimation and Compressive Sensing", *Signal Processing*, Elsevier, Volume 94, Jan. 2014, Pages 401–408.

[23] S. Stanković, I. Orović, and L. Stanković, "An Automated Signal Reconstruction Method based on Analysis of Compressive Sensed Signals in Noisy Environment", *Signal Processing*, Elsevier, Volume 104, November 2014, Pages 43–50.

[24] L. Stanković: "A measure of some time–frequency distributions concentration", *Signal Processing,* Vol. 81, No. 3, pp. 621-631, March 2001.

[25] S. Wong, E. Riseborough, G. Duff, "Experimental investigation on the distortion of ISAR images using different radar waveform", Defence R&D Canada – Ottawa, *Technical Memorandum*, September 2003.

[26] L. Stanković, S. Stanković, and M. Daković, "From the STFT to the Wigner distribution," *IEEE Signal Processing Magazine*, Vol. 31, No. 3, May 2014, pp. 163-174 (www.tfsa.ac.me/LN).

Ljubiša Stanković (Fellow IEEE) was born in Montenegro on June 1, 1960. He received the B.S. degree from the University of Montenegro, Podgorica, in 1982, the M.S. degree from the University of Belgrade, Belgrade, Yugoslavia, in 1984, and the Ph.D. degree from the University of Montenegro in 1988, all in electrical engineering. In 1982 he received the "Best Student at the University" award from the University of Montenegro. As a Fulbright grantee, he spent the 1984-1985 academic year at the Worcester Polytechnic Institute, Worcester, MA. Since 1982, he has been on the faculty at the University of Montenegro, where he has been a full professor since 1995. In 1997-1998 and 1999, he was on leave at the Ruhr University Bochum, Bochum, Germany, with Signal Theory Group, supported by the Alexander von Humboldt Foundation. At the beginning of 2001, he spent a period of time at the Technische Universiteit Eindhoven, Eindhoven, The Netherlands, as a visiting professor. During the period of 2003-2008, he was Rector of the University of Montenegro. He was also active in politics, as a vice president of the Republic of Montenegro from 1989 to 1991 and a member of the Federal Parliament of Yugoslavia 1992-1996. Prof. Stankovic is the ambassador of Montenegro to the United Kingdom, Republic of Ireland, and Iceland. He is also a vistiting academic at the Imperial College, London. His current interests are in time-frequency analysis, radar signal processing, and sparse signal processing. He published more than 350 technical papers, more than 130 of them in the leading international journals, mainly the IEEE editions. He published a book "*Time-Frequency Signal Analysis with Applications*", with Artech House in 2013. He authored several chapters in reference books and monographs published by Academic Press, Elsevier, and CRC. Prof. Stanković received the highest state award of the Republic of Montenegro in 1997, for scientific achievements. His group received a research award grant in 2001 from the Volkswagen Foundation, Germany. He was a member the IEEE Signal Processing Society's Technical Committee on Theory and Methods, and an Associate Editor of the *IEEE Transactions on Image Processing*, *IEEE Signal Processing Letters*, and *IEEE Transactions on Signal Processing*. Prof. Stankovic is a member of the National Academy of Science and Art of Montenegro (CANU) since 1996 and a member of the European Academy of Sciences and Arts.